Electronic Supplementary Material (ESI) for Environmental Science: Processes & Impacts.

Supporting Information for:

Crystal lattice defects in nanocrystalline metacinnabar in contaminated streambank soils indicate a role for biogenic sulfides in the formation of mercury sulfide phases.

Faye Koenigsmark[1], Michelle Chiu[2], Nelson Rivera[1], Alexander Johs[2], Jeremy Eskelsen[2], Donovan Leonard[2], Boakai K. Robertson[3], Anna Szynkiewicz[4], Christopher Derolph[2], Linduo Zhao[2], Baohua Gu[2], Heileen Hsu-Kim[1], Eric M. Pierce[2]*

[1]Civil and Environmental Engineering, Box 90287, Duke University, Durham, North Carolina 27708, USA

[2]Environmental Sciences Division, Oak Ridge National Laboratory, Oak Ridge, TN 37831, USA

[3]Department of Biological Sciences, Alabama State University, Montgomery, AL 36104, USA

[4]Department of Earth and Planetary Sciences, University of Tennessee at Knoxville, Knoxville, TN 37996, USA

Keywords: nanocrystalline metacinnabar, spectroscopy, mercury, speciation

***Corresponding author**: Phone: 865-574-9968, Email: pierceem@ornl.gov

Table of Contents

Section 1: Methods

Site Description

Fig. SI1. Samples were collected from the historical release deposit (dark-colored layers) of the exposed streambanks along EFPC. Shown in this figure is sample HRD-43R, located 18.2 km upstream of the mouth of EFPC.

Sulfur Sequential Extraction and Isotope Measurement

Sulfur sequential extraction method was used to extract various oxidation states of sulfur (SO_4^{2-}, S^0, S^-, S^{2-}) from the HRD soil samples selected for determination of the amount and isotope composition of sulfur ($\delta^{34}S$). Five gram aliquots of HRD soil samples were prepared by grinding the samples in an agate mortar and pestle. The elemental sulfur (S^0) was extracted from the soil using dichloromethane (DCM) in a Soxhlet apparatus held at 40°C for 12 hours. Activated copper granules were added to the sample flask to recover elemental sulfur as CuS. In a separate extraction apparatus, the copper granules were treated with 30 mL solution of hot deoxygenated 6 N HCl while bubbling the solution with N_2 gas, which released H_2S that reacted with $AgNO_3$ solution resulting in precipitation of Ag_2S.

Following DCM extraction, the residual soil was treated with 30 mL of 6 N HCl in the same way as the copper granules were. In this step, evolved H_2S from acid-volatile sulfur phase (S^{2-}) was also precipitated as Ag_2S. Additionally, dissolved iron was removed from the acid leachate by precipitation as

iron oxides following the addition of NaOH pellets to adjust the pH to 9 – 10. After the NaOH treatment and removal of iron oxides, the remaining solution was acidified to pH<3 with 12 N HCl and acid-soluble sulfate (SO_4^{2-}) was precipitated from the remaining solution as $BaSO_4$ by adding 1-2 mL of 10% barium chloride solution. In the last step, the remaining sediment was treated with a mixture of 20 mL in 12 N HCl and 20 mL of 1 M $CrCl_2 \cdot 6H_2O$ under N_2. This released H_2S from chromium-reducible sulfide phase (S^-) which was recovered as described above.

The amount (wt.% S) of SO_4^{2-}, S^0, S^-, S^{2-} phases was calculated based on the air-dried masses of $BaSO_4$ and Ag_2S relative to the dry mass of the soil sample used for extraction. The S isotope composition ($\delta^{34}S$) of $BaSO_4$ and Ag_2S was measured using a Costech elemental analyzer (EA) coupled with a Delta Plus XL isotope ratio mass spectrometer in the Stable Isotope Laboratory, University of Tennessee. Approximately 0.5 mg of $BaSO_4/Ag_2S$ was packed into a tin capsule with 1–5 mg of V_2O_5 to allow for a complete combustion of the sample inside the EA. Isotope data are reported with respect to VCDT (Vienna Canon Diablo Troilite). The correction was based on laboratory standards calibrated to the IAEA SO5, SO6 and NBS-127 standards. Analytical reproducibility was better than ±0.2% for standards and duplicate samples.

Bio-HgS Synthesis

Biotic HgS, referred to as bio-HgS, was extracellularly synthesized using sulfate-reducing bacteria, *Desulfovibrio desulfuricans* ND132 (culture collection number DSM 101870)[1]. *D. desulfuricans* ND132 was cultured anaerobically at 30 °C in a modified yeast extract medium (25 mL)[2–4], supplemented with 40 mM pyruvate and 20 mM Na_2SO_4 as the respective electron donor and electron acceptor. After 3 days incubation, the measured sulfide concentration was ~650 mg/L in the reactor. Sulfide concentrations were measured using colorimetric methods (or Hach Method 8131, Hach Inc., Loveland, CO). At this time, 0.05 mM anoxic $HgCl_2$ was added to form biogenic HgS precipitates. The HgS was then harvested from the reactor, rinsed with deoxygenated water, deposited on a TEM grid, and analyzed.

Section 2: Elemental Analysis

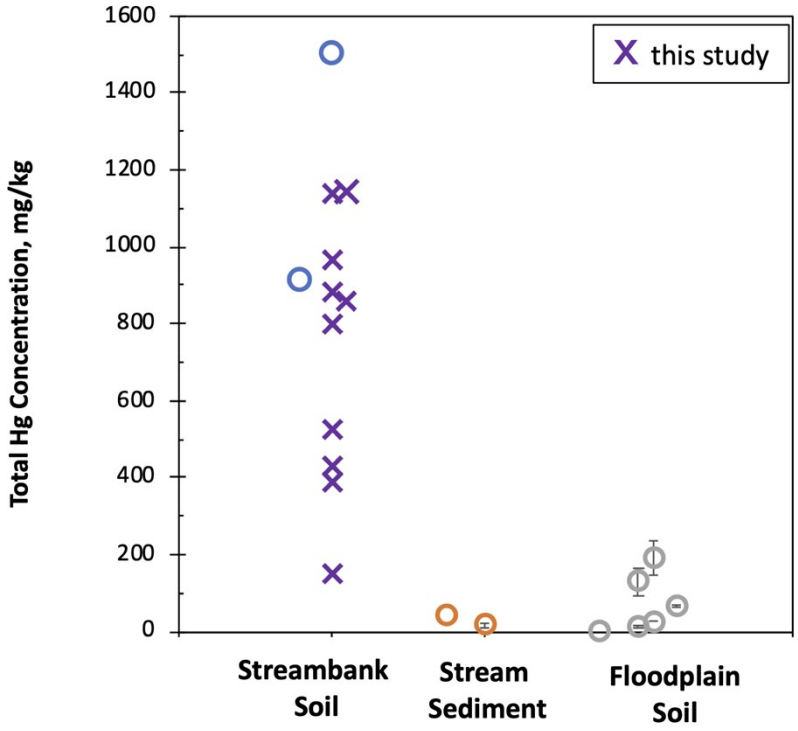

Fig. SI2. Average THg concentrations for streambank soils,[5,6] stream sediments,[6,7] and floodplain soils[6,8–11] in EFPC reported by previous studies. Purple (X) denote total Hg concentrations for streambank soils in this study.

Section 3: Microscopy and Spectroscopy

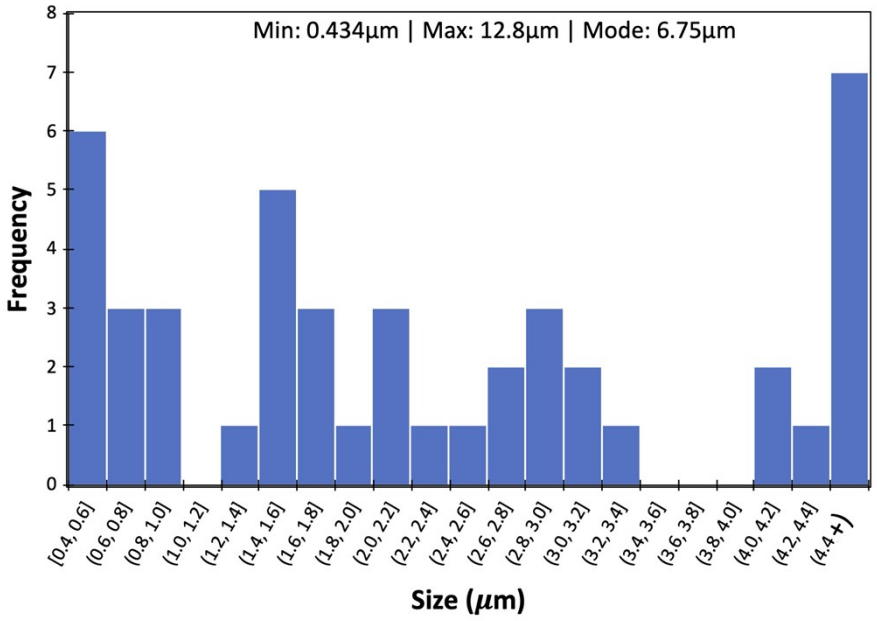

Fig. SI3. Size distribution of HgS aggregates (N = 45) measured by SEM from samples HRD-40R, -54L, -43R, -8R, -2L, -31L, -12R, and -22R.

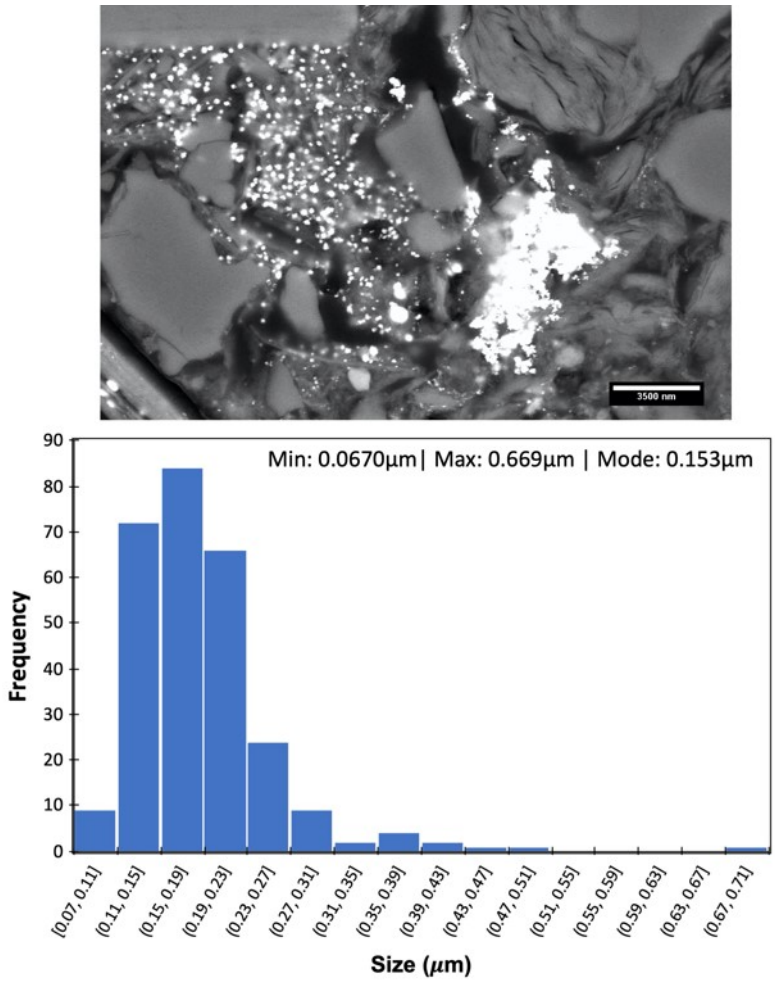

Fig. SI4. Size distribution of HgS aggregates (N =275) measured by SEM from one area of streambank sample HRD-2L.

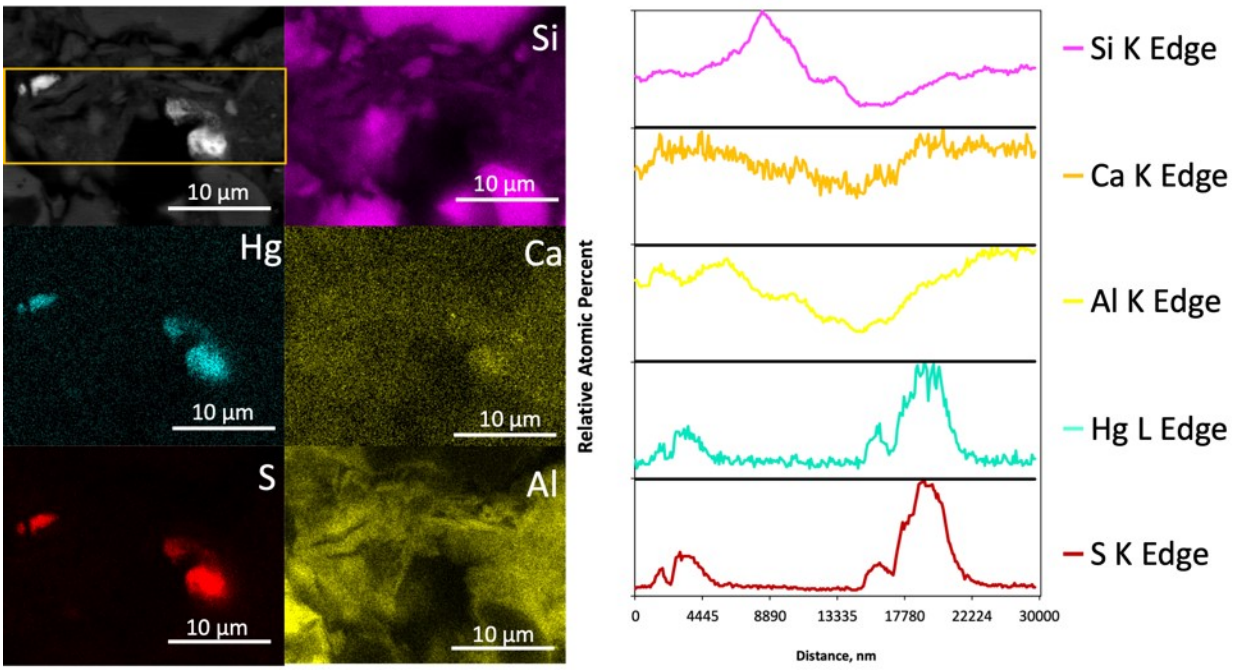

Fig. SI5. Left: EDS maps for streambank soil HRD-54 showing the presence of Al, Hg, Ca, S, and Si. Right: corresponding EDS average horizontal line for each element.

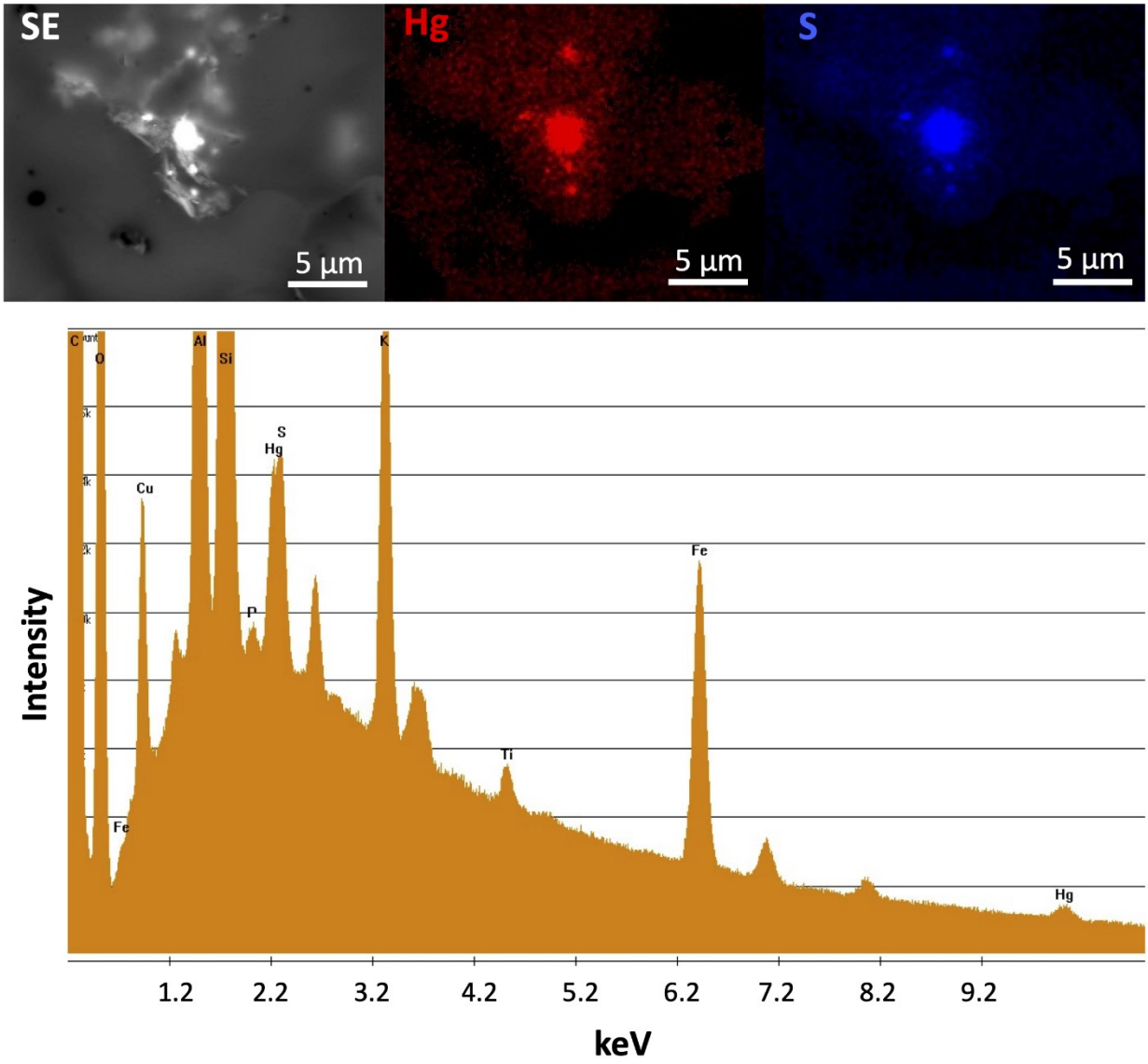

Fig. SI6. Streambank sample HRD-4L. Top: Secondary electron (SE) SEM imaging and EDS mapping indicating collocation of mercury (Hg) and sulfur (S). Bottom: Multi-element EDS spectrum for a spot analysis.

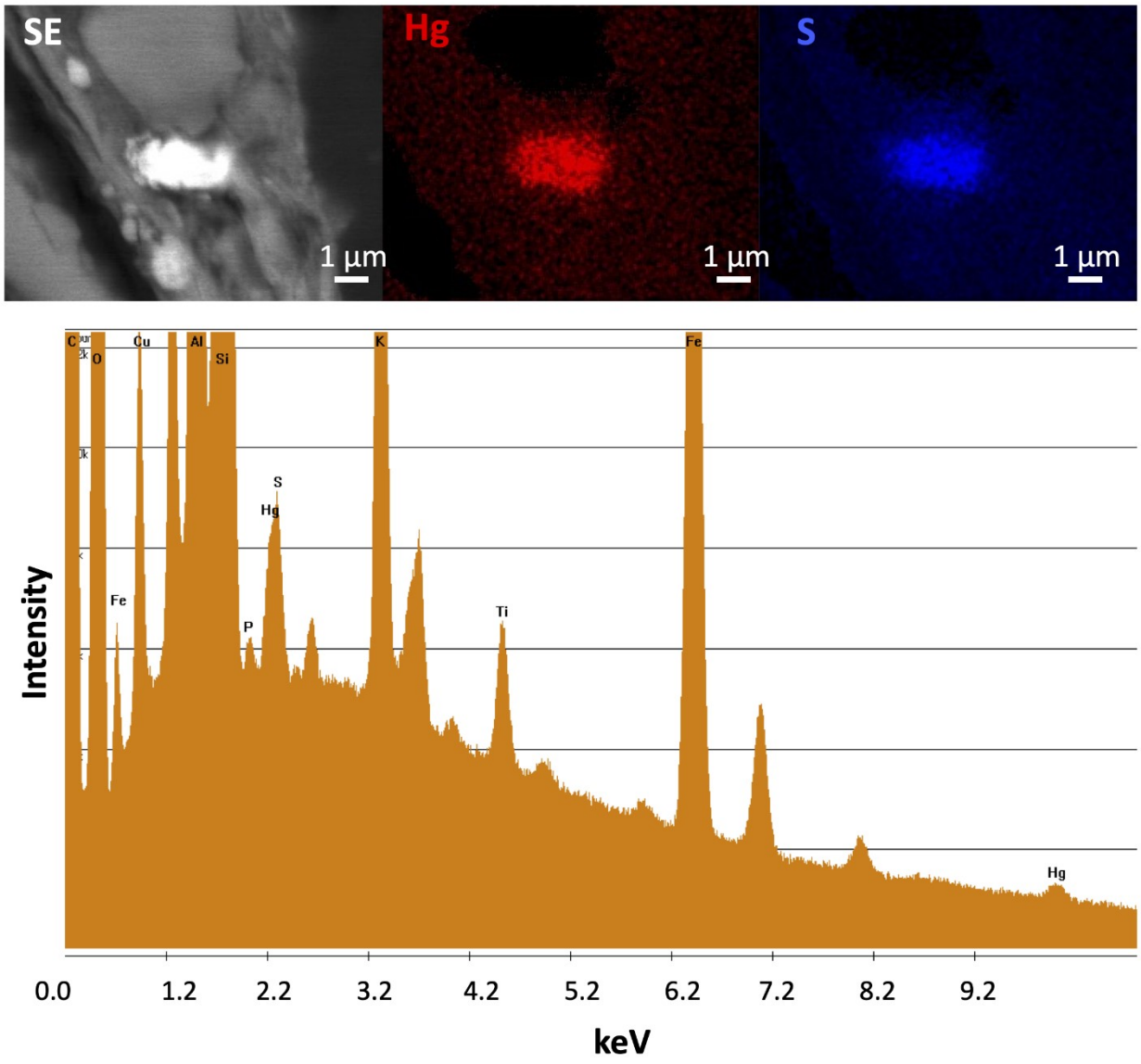

Fig. SI7. Streambank sample HRD-4L. Top: Secondary electron (SE) SEM imaging and EDS mapping indicating collocation of mercury (Hg) and sulfur (S). Bottom: Multi-element EDS spectrum for a spot analysis.

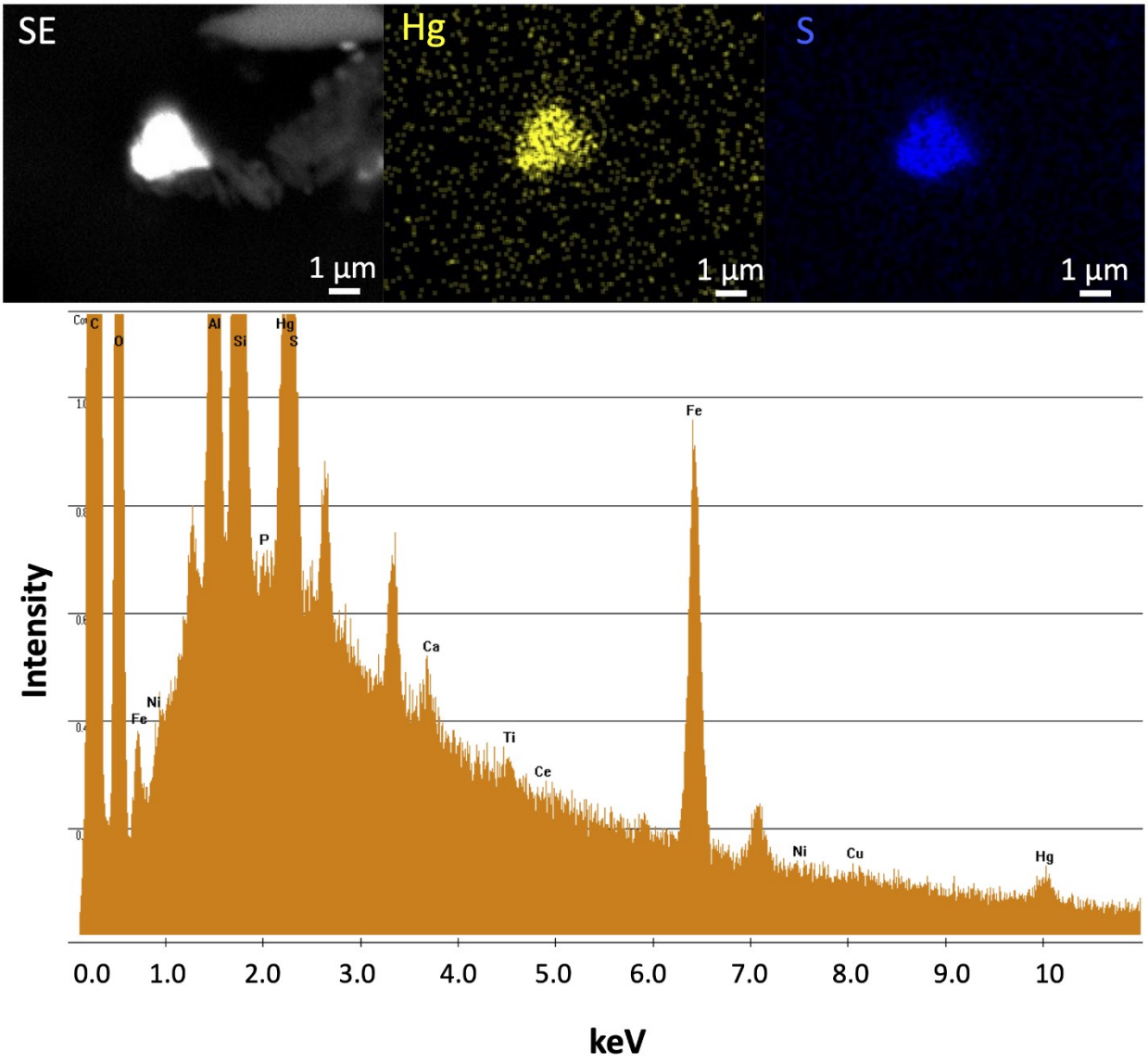

Fig. SI8. Streambank sample HRD-22L. Top: Secondary electron (SE) SEM imaging and EDS mapping indicating collocation of mercury (Hg) and sulfur (S). Bottom: Multi-element EDS spectrum for a spot analysis.

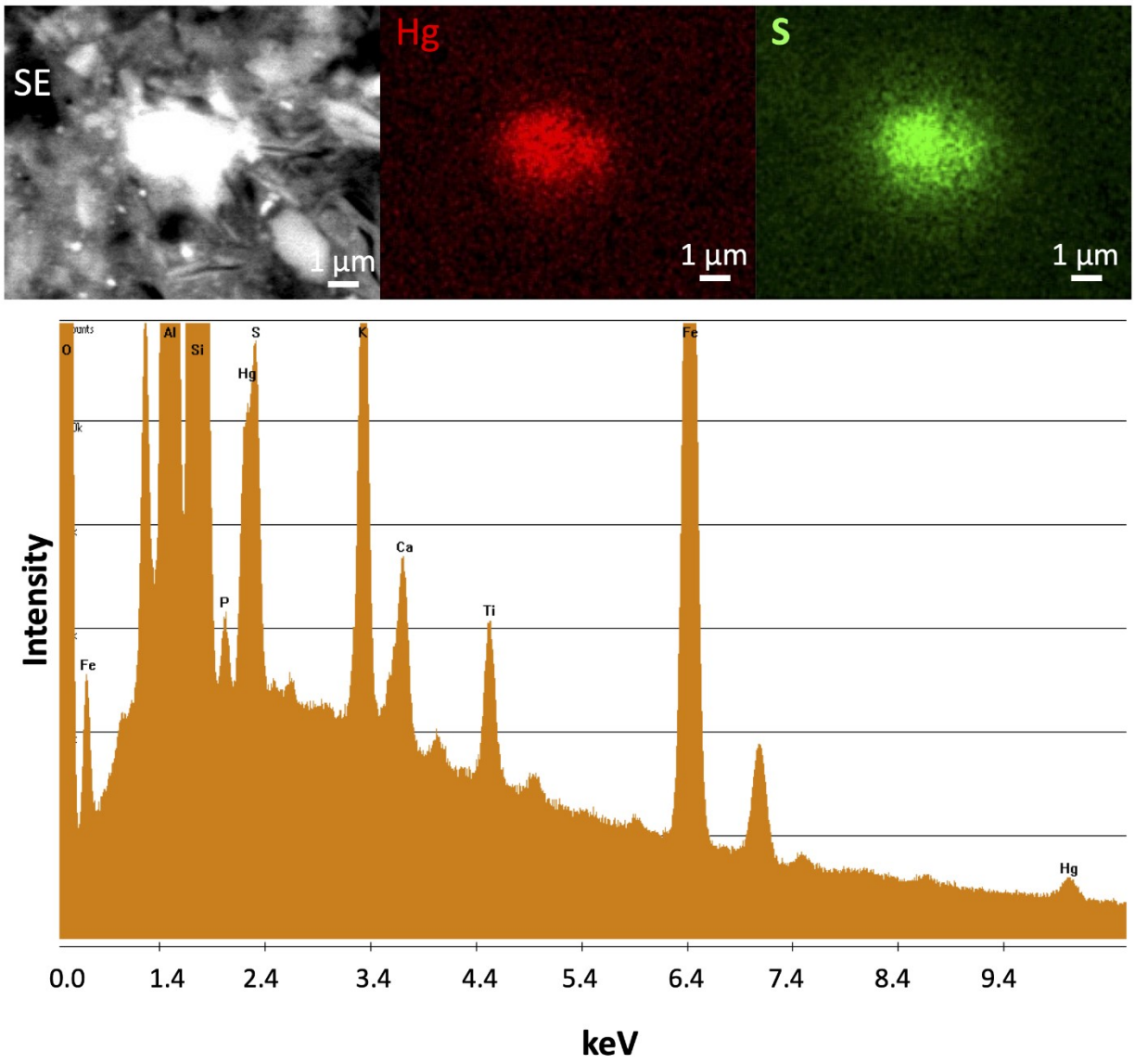

Fig. SI9. Streambank sample HRD-43R. Top: Secondary electron (SE) SEM imaging and EDS mapping indicating collocation of mercury (Hg) and sulfur (S). Bottom: Multi-element EDS spectrum for a spot analysis.

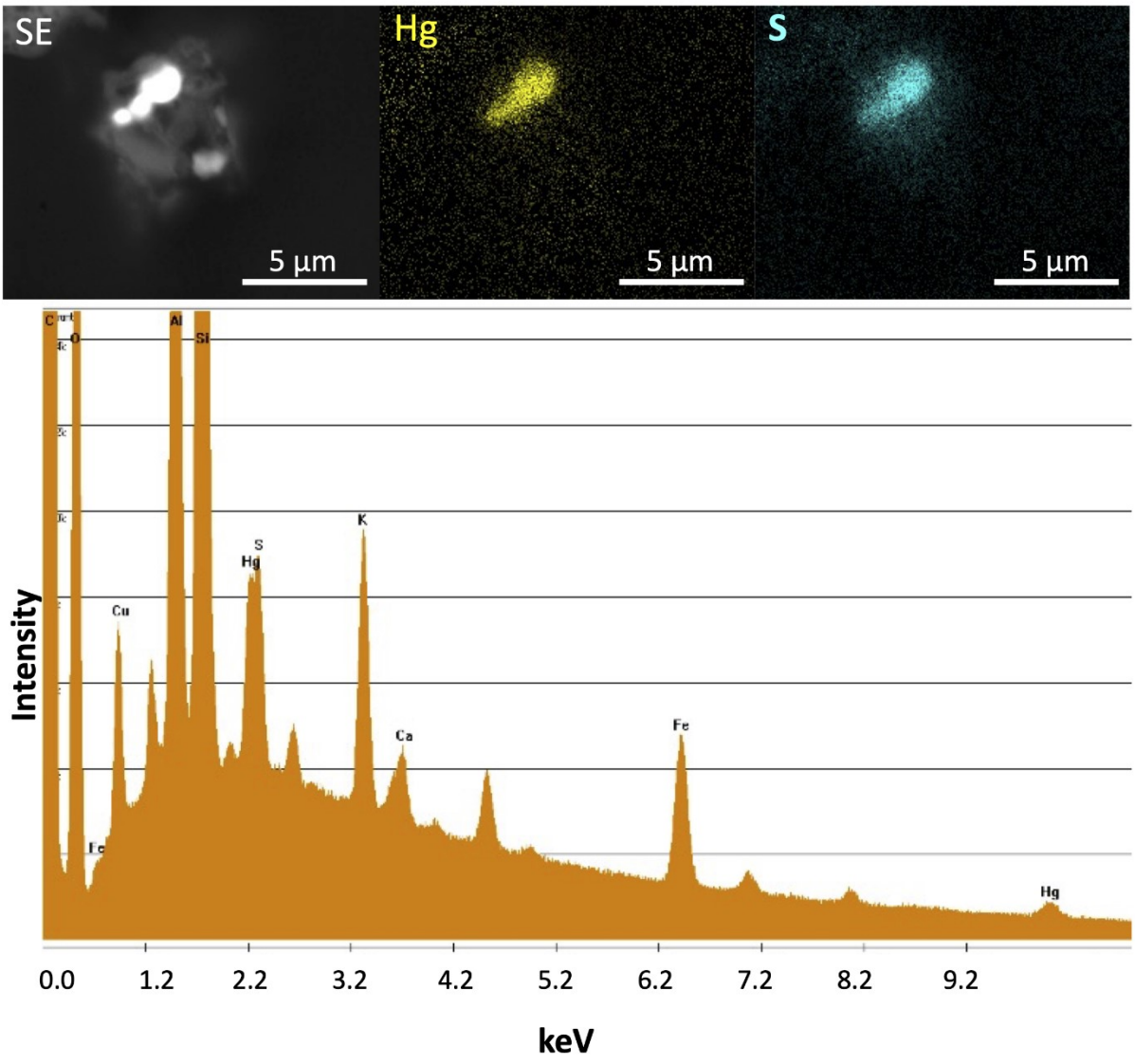

Fig. SI10. Streambank sample HRD-54L. Top: Secondary electron (SE) SEM imaging and EDS mapping indicating collocation of mercury (Hg) and sulfur (S). Bottom: Multi-element EDS spectrum for a spot analysis.

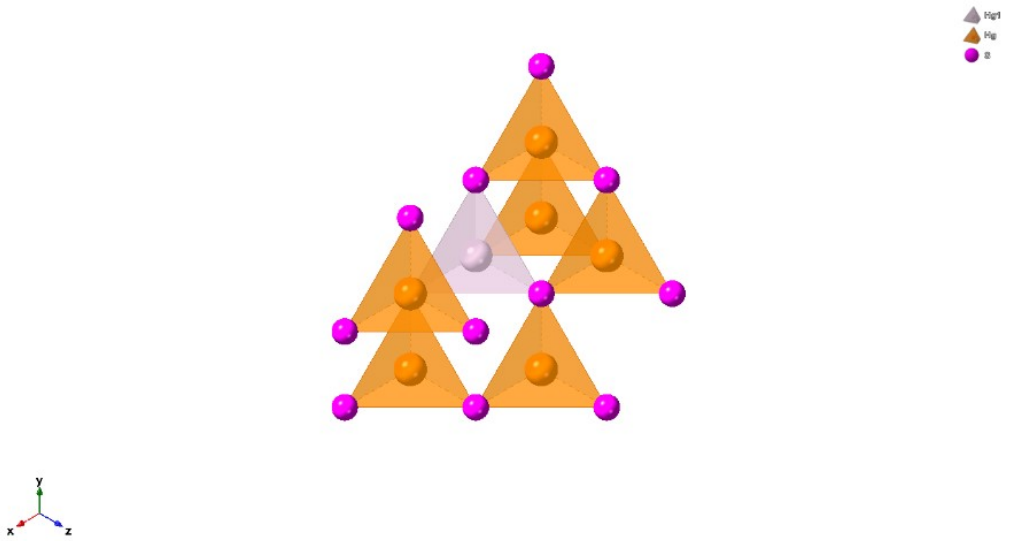

Fig. SI11. A HgS cluster generated from the fitted CNs in Table 2 with orientation along the 111 crystal plane. The grey central Hg atom is surrounded by 6 Hg atoms (orange). The mercury atoms are tetrahedrally coordinated to sulfur (pink). The HgS cluster measures ~1 nm in size. *Images and video generated using CrystalMaker®: a crystal and molecular structures program for Mac and Windows. CrystalMaker Software Ltd, Oxford, England (www.crystalmaker.com)*

Table SI1. Reference EXAFS parameters for fits to possible Hg compounds in EFPC soil environment. Where A-B is the absorber-backscatter atom pair; R is the interatomic distance between A and B; and N is the coordination number of backscatter atom.

Phase	A-B	N	R (Å)	Ref.
Nano-HgS (192 h old)	Hg-S	3.9 ± 0.4	2.53 ± 0.01	Pham 2014 [12]
Metacinnabar (β-HgS)	Hg-S	4	2.54	Pham 2014 [12]
	Hg-Hg	12	4.14	
	Hg-S	12	4.85	
	Hg-Hg	6	5.85	
Cinnabar (α-HgS)[12]	Hg-S	2	2.37	Pham 2014 [12]
		2	3.06	
		2	3.26	
	Hg-Hg	2	3.76	
		4	4.03	
		6	4.07	
Hg-thiol	Hg-S	2	2.33	Skyllberg 2006 [13]
	Hg-C(-S)	2.2	3.29	
Hg-organic soil	Hg-S	0.7-2.0	2.33-2.36	Skyllberg 2006 [13]
Mercury Chloride ($HgCl_2$ (s))	Hg-Cl	2	2.28	Serrano 2018 [14]
	Hg-Cl	6	3.36-3.46	
	Hg-Hg	4	4.33-4.41	
	Hg-Cl	6	4.58-4.84	
	Hg-Hg	4	4.86	
Montroydite (HgO)	Hg-O	2	2.05	Serrano 2018 [14]
	Hg-O	4	2.83	
	Hg-Hg	12	3.31-3.74	
	Hg-O	6	4.08-4.48	
	Hg-Hg	4	4.83	
Schuetteite ($Hg_3(SO_4)O_2$(s))	Hg-O	2	2.07,2.12	Serrano 2018 [14]
	Hg-O	4	2.46-2.75	
	Hg-S	1	3.38	
	Hg-S	1	3.68	
	Hg-Hg	3	3.49-3.56	
	Hg-Hg	2	3.71,	
	Hg-Hg	1	3.83	

Section 4: Metagenomic Sequencing and Analysis

Soil Microbiome Results

The shotgun metagenome data of the HRD soil sample contained 62,502,761 sequences (14.2 Gbps), 73.5% of these passed dereplication and quality control. The number of sequences containing ribosomal RNA genes was 77,716. The full dataset is available on MG-RAST under sample ID mgs812418.

The MG-RAST functional gene sequence analysis showed that Bacteria were the dominant domain representing 98.4% of sequences, whereas the Archaea and Eukaryota represented 0.69% and 0.71% of total sequences, respectively. The bacterial sequences are distributed across 35 different phyla. The most abundant phyla were the Proteobacteria with 54.6%, the Actinobacteria with 10.8% and the Acidobacteria with 8.5% of total sequences (**Fig. SI12**). Among the Proteobacteria, the most abundant classes were the Alphaproteobacteria with 20.7%, the Betaproteobacteria with 10.2%, the Gammaproteobacteria with 9.1% and the Deltaproteobacteria with 8.79% of total sequences.

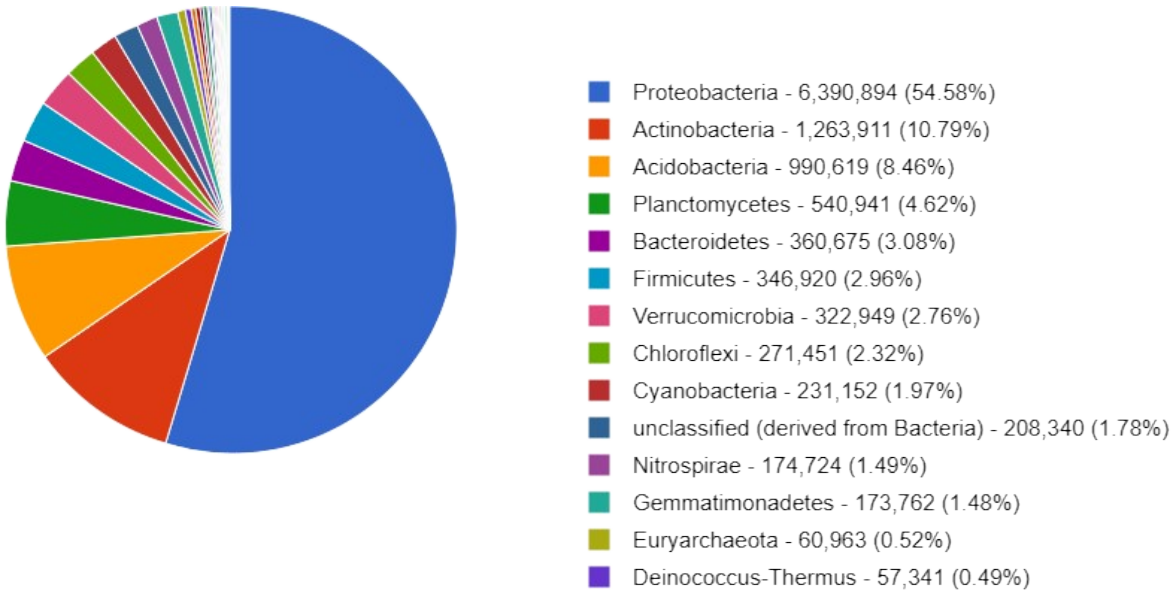

Fig. SI12. Distribution of taxa in EFPC HRD soil. Most abundant taxa in soil microbiome at the phylum level (top 14).

Table SI2. Lineages known to harbor sulfate-reducing microorganisms based on the distribution of dissimilatory (bi)sulfite reductase genes (reductive *dsrAB*) as a functional marker. Adapted from Müller et al.[15]

Domain	Phylum	Class	Order	Family	Genus
Archaea	Crenarchaeota	Thermoprotei	Thermoproteales	Thermoproteaceae	
Archaea	Euryarchaeota	Archaeoglobi	Archaeoglobales	Archaeoglobaceae	Archaeoglobus
Bacteria	Actinobacteria	Coriobacteriia	Eggerthellales	Eggerthellaceae	
Bacteria	Firmicutes	Clostridia	Clostridiales	Peptococcaceae	
Bacteria	Firmicutes	Clostridia	Thermoanaerobacterales	Thermoanaerobacteraceae	
Bacteria	Firmicutes	Clostridia	Thermoanaerobacterales	Thermodesulfobiaceae	
Bacteria	Firmicutes	Negativicutes	Selenomonadales	Sporomusaceae	
Bacteria	Nitrospirae	Thermodesulfovibrionia	Thermodesulfovibrionales	Thermodesulfovibrionaceae	Thermodesulfovibrio
Bacteria	Thermodesulfobacteria	Thermodesulfobacteria	Thermodesulfobacteriales	Thermodesulfobacteriaceae	
Bacteria	Proteobacteria	Deltaproteobacteria	Desulfarculales	Desulfarculaceae	
Bacteria	Proteobacteria	Deltaproteobacteria	Desulfobacterales	Desulfobacteraceae	
Bacteria	Proteobacteria	Deltaproteobacteria	Desulfobacterales	Desulfobulbaceae	
Bacteria	Proteobacteria	Deltaproteobacteria	Desulfovibrionales	Desulfohalobiaceae	
Bacteria	Proteobacteria	Deltaproteobacteria	Desulfovibrionales	Desulfomicrobiaceae	
Bacteria	Proteobacteria	Deltaproteobacteria	Desulfovibrionales	Desulfonatronumaceae	
Bacteria	Proteobacteria	Deltaproteobacteria	Desulfovibrionales	Desulfovibrionaceae	
Bacteria	Proteobacteria	Deltaproteobacteria	Syntrophobacterales	Syntrophaceae	
Bacteria	Proteobacteria	Deltaproteobacteria	Syntrophobacterales	Syntrophobacteraceae	

Section 5: SI References

1. Gilmour, C. C., Soren, A. B., Gionfriddo, C. M., Podar, M., Wall, J. D., Brown, S. D., Michener, J. K., Urriza, M. S. G. & Elias, D. A. Pseudodesulfovibrio mercurii sp. nov., a mercury-methylating bacterium isolated from sediment. *Int. J. Syst. Evol. Microbiol.* **71**, (2019).
2. Zhao, L., Chen, H., Lu, X., Lin, H., Christensen, G. A., Pierce, E. M. & Gu, B. Contrasting Effects of Dissolved Organic Matter on Mercury Methylation by Geobacter sulfurreducens PCA and Desulfovibrio desulfuricans ND132. *Environ. Sci. Technol.* **51**, 10468–10475 (2017).
3. Liu, Y. R., Lu, X., Zhao, L., An, J., He, J. Z., Pierce, E. M., Johs, A. & Gu, B. Effects of cellular sorption on mercury bioavailability and methylmercury production by desulfovibrio desulfuricans ND132. *Environ. Sci. Technol.* **50**, 13335–13341 (2016).
4. Hu, H., Lin, H., Zheng, W., Tomanicek, S. J., Johs, A., Feng, X., Elias, D. A., Liang, L. & Gu, B. Oxidation and methylation of dissolved elemental mercury by anaerobic bacteria. *Nat. Geosci.* **6**, 751–754 (2013).
5. Southworth, G. & Ketelle, R. *Sources of Mercury to East Fork Poplar Creek Downstream from the Y-12 National Security Complex : Inventories and Export Rates*. *Security* (2010).
6. Watson, D., Bevelhimer, M., Brandt, C., Derolph, C., Brooks, S., Mayes, M., Olsen, T., Dickson, J., Peterson, M. & Ketelle, R. *Evaluation of Lower East Fork Poplar Creek Mercury Sources–Model Update*. (2016). doi:ORNL/SR-2016/503.
7. Brooks, S., Eller, V., Dickson, J., Earles, J., Lowe, K., Mehlhorn, T., Olsen, T., Derolph, C., Watson, D., Phillips, D. & Peterson, M. *Mercury Content of Sediments in East Fork Poplar Creek: Current Assessment and Past Trends*. (2017). doi:ORNL/TM-2016/578.
8. Han, F. X., Shiyab, S., Chen, J., Su, Y., Monts, D. L., Waggoner, C. A. & Matta, F. B. Extractability and bioavailability of mercury from a mercury sulfide contaminated soil in Oak Ridge, Tennessee, USA. *Water. Air. Soil Pollut.* **194**, 67–75 (2008).
9. Poulin, B. A., Aiken, G. R., Nagy, K. L., Manceau, A., Krabbenhoft, D. P. & Ryan, J. N. Mercury transformation and release differs with depth and time in a contaminated riparian soil during simulated flooding. *Geochim. Cosmochim. Acta* **176**, 118–138 (2016).
10. Pant, P., Allen, M. & Tansel, B. Mercury contamination in the riparian zones along the East Fork Poplar Creek at Oak Ridge. *Ecotoxicol. Environ. Saf.* **74**, 467–472 (2011).
11. Revis, N. W., Osborne, T. R., Holdsworth, G. & Hadden, C. Distribution of mercury species in soil from a mercury-contaminated site. *Water. Air. Soil Pollut.* **45**, 105–113 (1989).
12. Pham, A. L. T., Morris, A., Zhang, T., Ticknor, J., Levard, C. & Hsu-Kim, H. Precipitation of nanoscale mercuric sulfides in the presence of natural organic matter: Structural properties, aggregation, and biotransformation. *Geochim. Cosmochim. Acta* **133**, 204–215 (2014).
13. Skyllberg, U., Bloom, P. R., Qian, J., Lin, C. M. & Bleam, W. F. Complexation of mercury(II) in soil organic matter: EXAFS evidence for linear two-coordination with reduced sulfur groups. *Environ. Sci. Technol.* **40**, 4174–4180 (2006).
14. Serrano, S., Vlassopoulos, D., Bessinger, B. & O'Day, P. A. Immobilization of Hg(II) by coprecipitation in sulfate-cement systems. *Environ. Sci. Technol.* **46**, 6767–6775 (2012).
15. Müller, A. L., Kjeldsen, K. U., Rattei, T., Pester, M. & Loy, A. Phylogenetic and environmental diversity of DsrAB-type dissimilatory (bi)sulfite reductases. *ISME J.* **9**, 1152–1165 (2015).